Analysis of Coupled Electromagnetic-Thermal Effects in Superconducting Accelerator Magnets

Egbert Fischer [1], Roman Kurnyshov [2] and Petr Shcherbakov [3]

[1]Gesellschaft fuer Schwerionenforschung mbH, Darmstadt, Germany
[2]Electroplant, Moscow, Russia
[3]Institute for High Energy Physics, Protvino, Russia, 142281

E-mail: E.Fischer@gsi.de

Abstract **- The planned facility FAIR will include 5 magnet rings including two superconducting synchotrons. The SIS100 synchrotron is the core component of the facility and will be equipped with 2 Tesla dipole magnets pulsed with 4 Tesla/s. The cable of the magnet coils is made of a hollow NbTi composite cable of about 7 mm outer diameter, cooled with two-phase helium flow at 4.5 K. We calculate the heat load, the eddy and the hysteresis losses, investigate the impact of the ramping on the magnetic field, on the safety margin of the conductor and the required cooling for all different elements of the magnet including the coil, the yoke, the bus bars and the beam pipe. This analysis is based on properties measured at cryogenic temperatures and fine detailed FEM models.**

Manuscript received November 23, 2007; accepted January 9, 2008.Reference No. ST22; Category 6.
Paper submitted to proceedings of EUCAS 2007; published in JPCS **98** (2008), paper # 012261

I. INTRODUCTION

The planned Facility of Antiproton and Iron Research (FAIR) at GSI Darmstadt [1] will provide high intensity primary and secondary beams of ions and antiprotons for experiments in nuclear, atomic and plasma physics. It will consist of 2 synchrotrons in one tunnel, SIS100 (100 Tm rigidity[2]), SIS300 (300 Tm rigidity), and several storage rings. This paper deals only with finite element investigations for the fast-ramped superconducting (SC) dipoles of the SIS100 synchrotron. The superferric magnets have to provide a maximum field of 1.9 - 2.1 T, a ramp rate of 4 T/s and a repetition frequency of 1 Hz at a temperature of 4.5 K. The magnets are called superferric as their field quality is determined by the pole shape, as in conventional magnets, but their coils are made of superconductiong wires.

The Nuclotron ring of the JINR Dubna was the starting point for the magnet design. In the preliminary R&D stage, the main operation criteria (magnet ac loss, magnetic field quality and mechanical stability of the coil) had been physically analyzed and numerically tested [2], including finite element calculations [3]. A real accelerator magnet uses different materials for

[1] This work is supported by EU FP6 Design study (contract 515873 – DIRAC secondary-Beams)
[2] The rigidity is given by the integral dipole strength of all dipoles;

different parts. The field in the iron and in the aperture is influenced by the 3D geometry of the yoke and the beam pipe structure as well as by the steel $B - H$ (induction – field) curves which are nonlinear and anisotropic, as the yoke is laminated. The duty cycle of the synchrotron is limited by the operation parameters of the magnets. These are defined by the heat load due to the eddy current and hysteresis losses, their impact on the magnetic field as well as on the safety margin of the superconductor. We have been using the finite element code ANSYS[3] to fully describe the 3D electromagnetic behavior of accelerator magnets, especially of the superferric type [4].

We present now the results of analogous calculations of eddy current and hysteresis loss for the actual design of a full-length SIS100 dipole model. The loss budget of the design elements will be defined for the most demanding operation mode proposed. Using the results of the electromagnetic field calculations we extend our analysis to investigate the thermal effects in the main construction elements of the magnet and estimate the temperature margins of the superconductor and of the cryo-pump functionality of the beam pipe. We describe the method of the coupled electromagnetic-thermal field calculations and present the obtained temperature field maps.

II. THE SUPERCONDUCTING DIPOLE

In the beginning of 2006, the required operation cycles for the SIS100 and the corresponding design parameters of the main magnets were actualized within the Baseline Technical Report (FBTR) [1]. Recently, alternative dipole versions were proposed to provide higher cycle repetition rates and a larger horizontal beam aperture (increased from 115 x 60 mm to 140 x 60 mm) [5]. The 2D cross section of the actual design for a SIS100 straight dipole model is presented in Figure 1. The right side shows the corresponding mockup manufactured to test: the lamination block package, the yoke fixed by welding stainless steel brackets to it, coil and cooling tubes positioning. The magnet has a two layer coil with 8 turns per layer providing a field of 2 Tesla at roughly 6.8 kA. Six horizontal slits are introduced in the lamination near the yokes end, designated to suppress the eddy current effects caused by the longitudinal field component. In the mockup four additional cooling tubes (4) are placed in the corners of the yoke providing, in combination with the two central tubes, various options for cooling tests.

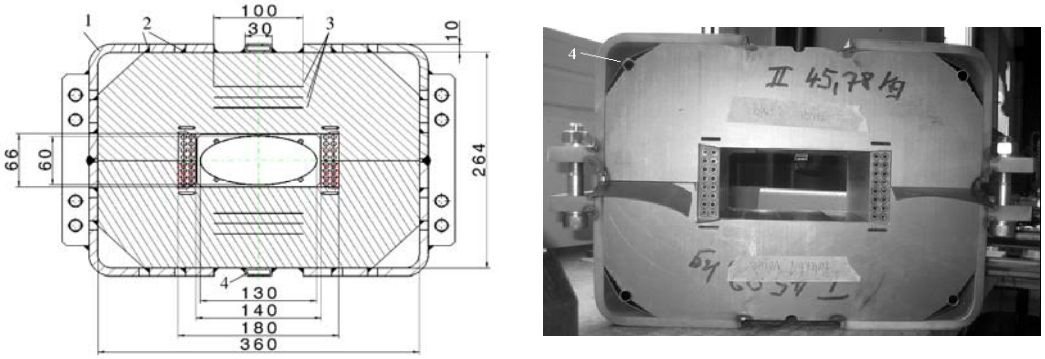

Fig. 1. Cross section of the straight dipole design with vacuum chamber (left), and the corresponding mockup for technological tests of the yoke fabrication and the coil fixation (right). Stainless steel brackets - 1, welding fixation - 2, horizontal slits - 3, yoke cooling tubes - 4. The coil turns consist of two vertical layers of 8 turns each.

[3] ANSYS is a commercial general finite element code developed by ANSYS, Inc.

Similar dipoles, but 1.4 m long and with the original Nuclotron aperture of 110 mm · 55 mm, have been already experimentally tested *via* calorimetric and magnetic field measurements [4]. Figure 2 shows a photo of the original Nuclotron dipole (left) and a 3D model of the new SIS100 dipole (right). The new dipole features a yoke, made of laminated electrical steel (1 mm thick), and brackets and end plates of stainless steel. The two layers of the coil are embedded in a G11 matrix. The vacuum chamber structure consists of an elliptical beam pipe (inner aperture: 130 mm · 60 mm, 0.3m thick stainless steel), cooling tubes and the mechanical stabilizing transversal ribs (1 mm thickness, 20 mm transposition pitch). The thermal contact between vacuum chamber, coil and yoke is provided by electrically insulating G11 plates.

The specific problems of finite element simulations for the real geometry of fast ramping superferric magnets, consisting of various ferromagnetic and nonmagnetic steels with a sophisticated 3D geometry, have been solved with ANSYS using edge elements. In preliminary methodical studies we had developed the approach for simplified models and verified them comparing our results to experimental data and to the results of other noncommercial codes. In a next step, the 3D short models for the dipole and the quadrupole had been thoroughly analyzed [3]. To construct an appropriate electromagnetic-thermal 3D model for the new SIS100 full size dipoles and for a correct FE analysis, the design details and material properties of the vacuum chamber are very important, as well as its connection to the coil and the yoke. The middle of the magnet is basically uniform in z, except for the rib structure of the vacuum pipe. Thus a magnet model with a length equal to the period of the rib structure was formed to reduce the number of elements. This required choosing correct boundary conditions, in particular enforcing eddy current traces always perpendicular to the cross section of our model. The 3D magnetic and the thermal models of magnet centre, equal to one period of the vacuum chamber with ribs, are shown in Figures 3 and 4.

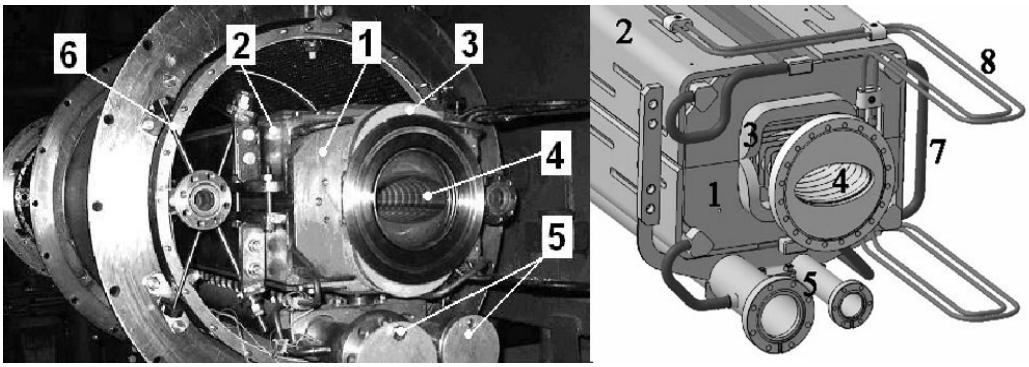

Fig. 2. View of the Nuclotron dipole inside the cryostat (left) and of the 3D model of the new SIS100 dipole (right): 1 - yoke end plate, 2 - brackets, 3 - coil end loop,4 - beam pipe, 5 - helium headers, 6 - suspension, 7 - yoke cooling tube, 8 - bus-bars

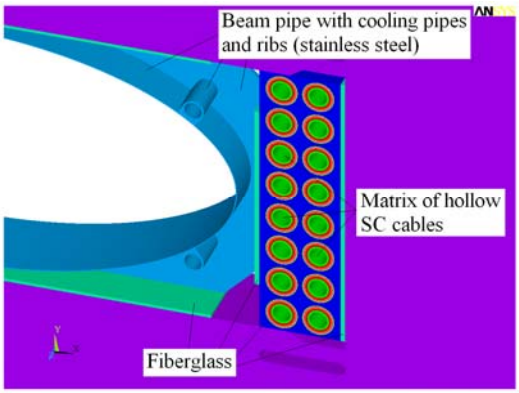

Fig. 3. Layout of the main parts of the SIS100 dipole FE model.

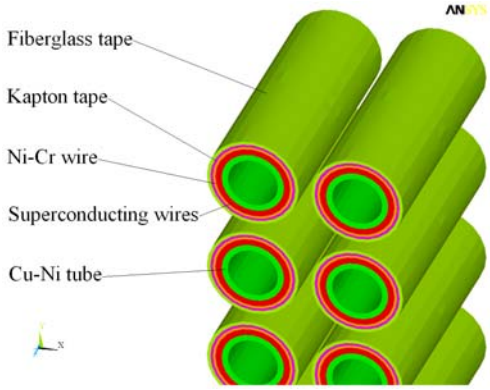

Fig. 4. Layout of the turns of the SC coil of the SIS100 dipole magnet.

A triangular cycle, continuously ramping with 4T/s between the injection field B_{min} = 0.24 T and B_{max} = 2.1 T, is actually the most demanding operation mode for the SIS 100 dipoles [5]. For our analysis we use here the approximation B_{min} = 0 T and a fixed current ramp $|dI/dt|$ = const with a cycle repetition rate of 1Hz. The thermal calculations are done using the time-averaged power of the AC loss. The inaccuracy of the so calculated results was estimated to be less then the uncertainties caused by the variation of the material data, *i.e.*, $dB(I)/dt$ is especially sensitive to the material properties $B(H)$ and the real packing factor of the yoke. Following the method given here, the exact calculation will be straight forward for all required cycles and all different magnet sizes.

III. AC LOSS RESULTS OF THE ELECTROMAGNETIC MODEL

The heat sources for the thermal calculations are the magnetic hysteresis and the eddy current loss in the structures of the yoke, the SC coil and the vacuum chamber. The hysteresis loss per cycle is not frequency-dependent and can be determined in the static magnetic mode. The eddy current loss was calculated as a transient process. We use the specific data and methods given in [6, 7] for calculating the hysteresis loss in the laminated yoke and in the superconducting multifilamentary wires. The applied electrical resistivities of the conductive materials at 4.2 K are provided in Table 1. The AC loss was integrated over all elements to obtain the contribution of each design unit of the magnet. The main loss sources are summarized in Table 2. The coil loss data are strongly dependent on the SC wire design. The upper extremes of the loss values for the SC coil are given for the wires already tested with a filament diameter of 6 μm, the lower values are estimated for wires with 2.5 μm filaments. The total values include also the eddy losses in the brackets (0.076 W/m) and the yoke cooling pipe (0.0067 W/m). The loss in the ribs of the vacuum chamber (0.097 W/m) is also negligible as well as the value obtained for the CuNi tubes of the cable (0.021 W/m). To estimate the total thermal loss of the dipole, to be cooled at 4 K, one also has to consider the end field effects (~ 5 W/dipole) and the static heat load.

Table 1. Resistivity of materials at 4.2 K, 10^{-7} Ohm·m

Electrical steel	Stainless steel	Copper	CuNi	NiCr
3.2	5	0.017	1.4	12

Table 2. Loss per cycle in the different parts of the magnet (for a lamination packing factor of 98%)

	Yoke assembly		Vacuum chamber		SC coil	
	Yoke Hysteresis	Yoke Eddy currents	Elliptical tube	Cooling pipes	Hysteresis in filaments	Eddy in matrix
AC loss, J/m	9.63	0.34	5.18	4.83	2.03-4.1	3.13-6.3
Total	10.05		10.1		5.18-10.4	

IV. THERMAL ANALYSIS

All thermal contacts between the different electrical conducting or insulating materials of the dipole construction, including the fine structure of the SC cable had been modeled thoroughly. The temperature boundary conditions are chosen to be T = 4.5 K at all inner surfaces of the cooling tubes; the heat flow from surfaces in contact with vacuum was approximated to be zero. The temperature dependence is considered for the thermal properties of all materials (thermal conductivity and specific heat capacity). Some characteristic values of the thermal conductivity and the specific heat capacity at 4.2 K are given in Table 3.

Table 3. Thermal conductivity λ and specific heat C of materials at 4.2 K.

	Electrical steel	Stainless steel	Copper	CuNi	G11	Kapton
λ, W/(m·K)	0.8	0.21	630	1.30	0.08	0.012
C, J/(kg·K)	0.4	2.1	0.1	0.11	1.55	0.8

The thermal analysis can be carried out in transient or steady state mode, but most of the analysis was performed in steady state mode due to the stable cycle repetition frequency of 1 Hz. The transient calculations, using the time-averaged loss power density, had shown that the steady state is achieved after approximately 60 cycles. The time-averaged AC power loss density function was applied to the thermal model and the steady state thermal problem was solved. To check the cryo-pump functionality of the beam pipe, the 3D distributions of the temperature was analyzed for different versions of the vacuum chamber construction: (I) for the complete chamber assembly, (II) with the ribs, but without cooling pipes, and (III) the beam pipe with cooling tubes but without ribs. The results are presented in Figures 5a, 6a, and 7a for the dipole. The transversal temperature profiles of the beam pipe in the plane of the rib are given in Figures 5b, 6b and 7b starting from the small half axis to the large half axis. The maximum temperatures are 11.5 K 13 K and 24.1 K for version I, II and III respectively. The corresponding values between the ribs are 15.3 K, 17.3 K and 24.1 K.

This small difference of the data for version I and II suggests, that the thermal contact of the vacuum chamber to the coil and the yoke cools the beam pipe more efficiently than the given cooling tube arrangement. This result is also important for the heat flow balance between the iron yoke and the coil. That finally defines the operation temperatures of the superconducting cable and its temperature margin.

I II III

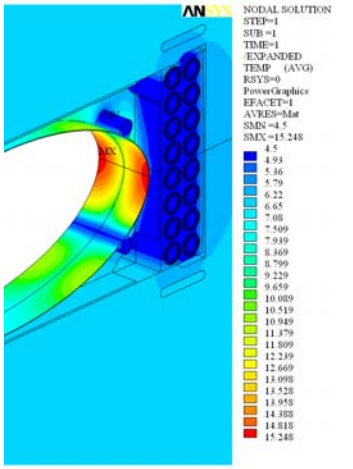

a)

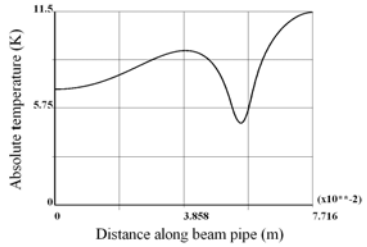

b)

Fig. 5. a) Temperature field for version I. b) Midplane inner temperature profile.

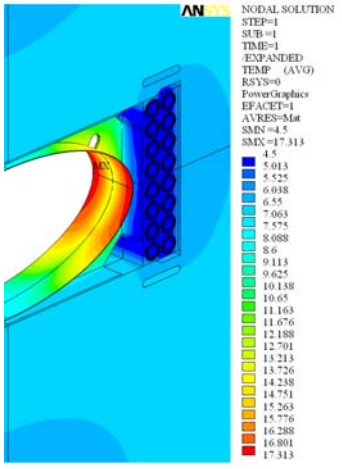

a)

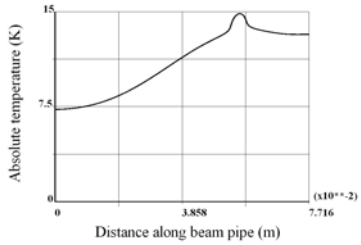

b)

Fig. 6. a) Temperature field for version II. b) Midplane inner temperature profile.

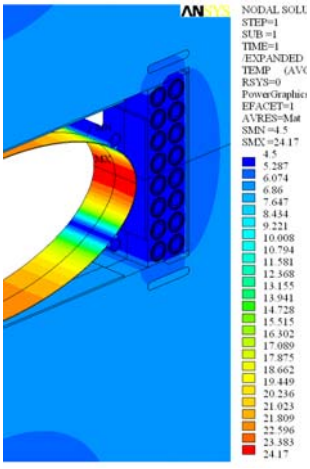

a)

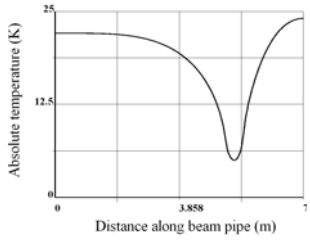

b)

Fig. 7. a) Temperature field for version III. b) Midplane inner temperature profile.

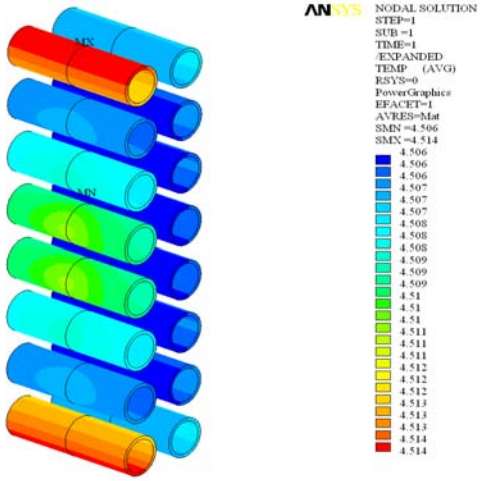

Fig. 8 a) Temperature field in the SC wires of coil turns (see Fig.4).The CuNi tubes, on which the wires are placed, are not shown.

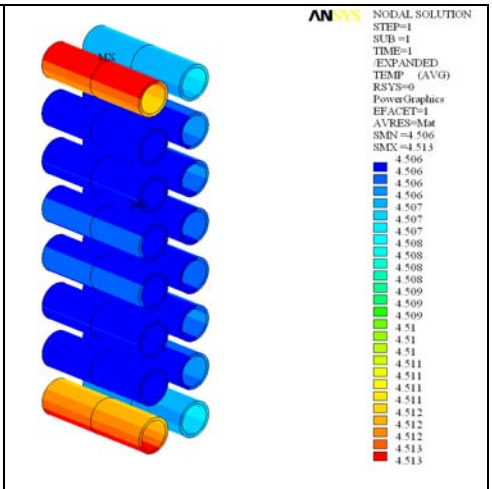

Fig. 8 b) Temperature field in the coil for a vacuum chamber design without ribs.

The temperature distribution in the superconducting wires, modeled by a cylindrical layer in the hollow superconducting cable, is presented in Figure 8 for the two different versions I and III. The CuNi tubes are not shown, but can be seen in Fig.4, showing a model of the cables and the support structure of the coil. It has been obtained from these

calculations, that the temperature gradient between the SC wires layer, contacting the outer surface of the CuNi tube, and the inner site of this tube, contacting the flowing helium at 4.5 K, is in the order of 0.01-0.03 K.

Taking into account the additional temperature drop between the CuNi cooling tube and the two-phase helium flow as well as the complicated fine structure of the contact surface of the 31 superconducting wires the experimental values should be slightly higher. A maximum temperature difference of 0.2 K was measured in special experiments on Nuclotron dipoles [8]. This shows that the temperature margin of the SC wire is defined by the temperature profile of the two-phase helium flow depending on the operation modes.

V. SUMMARY

A new electromagnetic-thermal 3D-FE model for superferric magnets was developed, including the periodical structure of the vacuum chamber cooled by forced two-phase helium flow. Special attention was paid to the modeling of the thermal contacts between the cable turns of the superconducting coil and the heat exchange between the coil and the laminated iron yoke. The hysteresis and the eddy current losses in the yoke, the vacuum chamber and the coil assemblies were calculated in static and transient modes. The obtained heat loads had been coupled with the simulation of the thermal processes to obtain the steady state thermal field distribution. The temperature distribution was calculated for the main design elements of the dipole and their detailed fine structure considering the planned operation modes of the magnets. The cryocooling efficiency of the vacuum chamber is extremely sensitive to the real heat transition between the beam pipe, the cooling tubes, the mechanical stabilizing ribs and their thermal contact to the coil structure and the yoke. Thus details of the manufacturing technology can cause a beam pipe temperature higher than the required limits. The calculations had shown that the cooling tubes placed on the beam pipe are inefficient in a realistic heat transfer regime. Consequently the additional heat flow from the vacuum chamber to the coil and the yoke should have a significant impact on the stability margins of the superconductor and on the operation cycle intensity of the whole accelerator.

In a next R&D step we plan to complete our FEM tools for mechanical calculations and also to combine the thermal analysis with detailed hydraulic investigations for the forced two phase helium flow cooling the coil and the beam pipe.

REFERENCES

[1] FAIR Baseline Technical Report 2006 (GSI Darmstadt) http://www.gsi.de/gsi-Future; see also this Forum, Reviews CR2 and CR4.

[2] E. Fischer et al., "Status of the Design of a Full Length Superferric Dipole and Quadrupole Magnets for the FAIR SIS100 Synchrotron", *IEEE Trans. Appl. Supercond.* **17**, 2, pp 1078-1082 (2007)

[3] E. Fischer, R. Kurnyshov and P. Shcherbakov, "Finite element calculations on detailed 3D models for the superferric main Magnets of the FAIR SIS 100 Synchrotron", (CHATS-AS 2006, Berkeley), *Cryogenics* **47**, 583-594 (2007)

[4] E. Fischer et al., "Analysis of the superferric quadrupole magnet design for the SIS100 accelerator of the FAIR project", EPAC 2006, Edinburgh, WEPLS091.

[5] E. Fischer, H. Khodzhibagiyan and A. Kovalenko, "Full size model magnets for the FAIR SIS100 Synchrotron", presented on MT-20, Philadelphia,2007, to be published.

[6] P. Shcherbakov et al., "Magnetic properties of silicon electrical steels and its applications in fast cycling SC magnets at low temperatures", RUPAC, 2004, Dubna, pp 298-300.
[7] Annex to Design Requirements and Guidelines Level 1 (DRG1) ITER Superconducting Material Database, article 5. Thermal, Electrical and Mechanical Properties of Materials at Cryogenic Temperatures N 11 FDR 42 01-07-05 R 0.1, http://www.iter-nl.nl/ITER_FDR/ .
[8] H. Khodzhibagiyan et al. 2003 "Design of new hollow superconducting NbTi cables for fast cycling synchrotron magnets", *IEEE Trans.Appl.Supercond*. **13**, N2, pp.3370-3373.